A microfluidic chip with poly(ethylene glycol) hydrogel microarray on nanoporous alumina membrane for cell patterning and drug testing

Zong-Bin Liu[a], Yu Zhang[b], Jin-Jiang Yu[a], Arthur Puk-Tat Mak[a], Yi Li[b] and

Mo Yang[a*]

[a]Biomedical Sensor and Nanotechnology Laboratory, Department of Health Technology and Informatics, the Hong Kong Polytechnic University, Hung Hom, Kowloon, Hong Kong

[b] Institute of Textiles and Clothing, the Hong Kong Polytechnic University, Hung Hom, Kowloon, Hong Kong

*Corresponding author: Dr. Mo Yang, Department of Health Technology and Informatics, the Hong Kong Polytechnic University, Hung Hom, Kowloon, Hong Kong, P.R. China.

E-mail: htmems@polyu.edu.hk; Phone: 852-2766-4946; Fax: 852-2334-2429

Abstract

In this paper, a microfluidic silicon chip with poly(ethylene glycol) (PEG) hydrogel microarray on the nanoporous anodized aluminum oxide (AAO) membrane was fabricated to form cell based microarray with controlled drug delivery. The PEG hydrogel microstructures were fabricated using photolithography on nanoporous alumina surface modified with a 3-(Trimethoxysilyl)propyl methacrylate (TPM) monolayer. During the photopolymerization reaction, 10x10 hydrogel microwell arrays were covalently bonded to the substrate via the TPM monolayer for cell patterning. Human KYSE-30 esophageal squamous epithelial cancer cells were shown to selectively adhere on the TPM modified alumina surface inside the microwells. The diffusion studies for the anti-cancer drug molecule of cisplatin were carried out for the microfabricated membrane array using a mini-diffusion chamber. The diffusion curves for the pore size of 25 nm and 55 nm showed different release profiles. Then, the drug testing experiment with cisplatin was explored using the microfabricated membrane array with the pore size of 55 nm for testing the drug effects on the KYSE-30 cancer cells. The cytotoxic effects of cisplatin on cancer cell number and cell morphology within microwells were explored based on this cell microarray.

Key words: Nanoporous alumina membrane; Drug release; Cisplatin; Poly(ethylene glycol) (PEG); Cell based microarray

1 Introduction

Cells usually integrate and respond to the surrounding environment such as chemicals and biomolecules in the fluids, physical properties (i.e. mechanical properties) of the substrates, and interactions between neighboring cells [1-2]. The ability to engineer cell-surface interactions for cell patterning and control sampling of analytes is important to study the effects of the microenvironment on cellular behavior [2-3].

Inorganic nanoporous alumina membrane, fabricated by electrochemical anodization technique, is a kind of material with self-ordered nanopores [4]. The nanopores diameter and length can be precisely controlled by the established fabrication process [5-9]. Due to its well-defined pore size and high pore density, nanoporous alumina membrane has been used for a wide of applications such as nanomaterial preparation [10], solution control regulation [11], DNA filtering and detection [12-14]. Recently, the controlled drug molecule release using alumina membrane was also explored for potential immunoisolation application [15]. Furthermore, due to its good biocompatibility, alumina membrane has already been used as a good substrate for cell culture [16] and tissue constructs [17]. These features make the nanoporous alumina membrane to have excellent potential for drug sampling devices in cellular behavior study. However, there are few examples to explore the possibility of generating cell based microarray on nanoporous alumina membrane which can be a potential *in vitro* analysis system for cell drug interaction due to the well defined diffusion transport effects of nanopores.

In this study, nanoporous alumina membrane was integrated with hydrophilic poly(ethylene glycol) (PEG) hydrogel layer by photolithography for the controlled delivery of specific anti-cancer drug cisplatin to the adherent cancer cells on the alumina membrane. In order to make PEG hydrogel attach on the nanoporous membrane, the alumina substrate was first grafted with a silane monolayer, which could covalently bond with PEG hydrogel during photo-polymerization process. The hydrophobic silane monolayer could also improve protein and cell attachment on the alumina surface which was not covered by PEG layer. Thus, cancer cell microarrays could be formed on the cell adhesive nanoporous alumina membrane surrounded with cell repelling hydrogel regions. A mini diffusion chamber with two compartments separated by the microfabricated membrane array was used for the diffusion experiments with the model anti-cancer drug cisplatin. During the drug testing experiments for KYSE-30 cancer cells, the concentration of cisplatin on the compartment with adherent cancer cells was controlled by the diffusion through the membrane. Adherent cancer cell number within the microwells and cell morphology change under the diffusion of cisplatin was also monitored.

2. Materials and Methods

2.1 Materials

Acetone, oxalic acid, chromic acid, phosphoric acid, 3-(Trimethoxysilyl)propyl methacrylate (TPM), poly(ethylene glycol) diacrylate (PEGDA, average Mn=700),

toluene, methanol, hydrogen peroxide were obtained from Sigma-Aldrich (St. Louis, USA). Irgacure 2959 was provided by Ciba Specialty Chemicals Inc (USA). Fibronectin and Bovine serum albumin (BSA) was purchased from Roche Inc (Germany).

2.2 Fabrication of nanoporous alumina membrane on silicon substrate

The fabrication of nanoporous alumina membrane on a silicon substrate was based on the anisotropic silicon etching and the two-step anodization of deposited aluminum thin film [8-9]. The whole process is shown in Fig. 1.

For the first step of fabrication of silicon microfluidic structure, a pre-cleaned 4 inch silicon (Si) wafer with a low stress silicon nitride layer on both sides was used as the starting substrate. First, Si_3N_4 on the back side was patterned using photolithography following by reactive ion etching (RIE) to open windows for microwells. Then, 30% potassium hydroxide (KOH) solution was used as the wet etchant to etch through the back side of the Si substrate at 80^oC until it reaches the etch-stop Si_3N_4 layer. KOH preferentially etches <100> crystal plane, resulting in a "V-groove" with the inward slope angle of 54.7^0.

Then, a thin layer of aluminum (Al) of 1000 nm was deposited onto the front side of the Si substrate by magnetron sputtering (90w, power density $3.8w/cm^{-2}$) using a 99.999% Al target in the atmosphere of research-grade Ar at $4x10^{-4}$ Torr. The deposition rate was 1 nm/s. The samples were mounted on a rotating stage to ensure

an even coating of the Al layer. The aluminum layer was then anodized following the standard two-step anodization procedures to form nanoporous membrane. The first anodization process was performed at 5^{o}C for 10 min under DC voltage (50V) in 0.3 M oxalic acid. The aluminum layer on the front side of the substrate was used as anode while Pt sheet was used as cathode. The solution was stirred in order to accelerate the dispensation of the generated heat. Then, the substrate was rinsed with distilled (DI) water and immersed into 4 wt% chromic acid and 8 wt% phosphoric acid in the etching step for 5 minutes. The second anodization step was then repeated at 50V for 8 min in 0.3 M oxalic acid solution at 5^{o}C. After the second anodization, the silicon nitride membrane support was removed by RIE etching. Alumina barrier layer removal and pore widening were followed in 8 wt% phosphoric acid for 5 to 20 minutes at room temperature dependent of the desired pore size. It was important to keep the silicon nitride membrane support before the anodization which could obviously keep the aluminum and alumina film intact before and after anodization. If silicon nitride support membrane on the backside was removed before anodization, the alumina layer was easy to break or detach from the substrate during anodizaiotn process and the successful rate was much lower.

2.3 Silane modification of the nanoporous alumina surface

Recently, silane treatment has been used for surface modification of alumina [18-20]. The fabricated nanoporous alumina membranes were boiled in 30%

hydrogen peroxide for 30 min to clean the surface. This step introduced OH groups on the nanoporous alumina surface which facilitated subsequent silane modification by TPM. For the formation of TPM monolayer, the nanoporous alumina surfaces were immersed into a 5% (V/V) solution of TPM in anhydrous toluene at 50^0C for 24 h. Then the alumina surfaces were washed by toluene followed by methanol and deionized water. The alumina surfaces were further air dried.

2.4 Fabrication of PEG hydrogel microstructures on AAO surface

PEG hydrogel microstructures were fabricated with PEG-DA by photopolymerization. In this experiment, a SU-8 chamber was first fabricated on the alumina surface of the chip. A 50 μm SU-8 2050 photoresist layer was coated on the alumina surface with the speed of 3000 rpm for 90s using a spin coater. Then the SU-8 layer was pre-baked at 65^oC for 3min and 95^oC for 9 min to evaporate the solvent. The sample was then UV exposed using a photomask with a square pattern at 10mW/cm^2 for 70s. Post exposure was carried out at 65^oC for 1 min and 95^oC for 7 min. The substrate was then developed in PGMEA (propylene glycol monomethyl ether acetate) from Microchem for 20 min, washed with isopropyl alcohol, and dried with a nitrogen gun. After developing, the unexposed center area was removed from the alumina surface and the SU-8 chamber was built.

Then, the PEG gel precursor was prepared by dissolving 20 mg Irgacure 2959 (photo-initiator) in 15 mL of PEG-DA solution. Thes precursor solution with 1.5 ml

was then injected into the pre-fabricated SU-8 chamber. A glass slide was used to cover the chamber and a photomask with the desired pattern was put onto proximity of the gel precursor. The solution was then exposed to UV light with the energy of 30mW/cm^2 for 90s using a 365 nm, UV spot curing system (EXFO, S1000 Omnicure, Canada). The exposed regions became insoluble and the desired microstructures were achieved by washing away the unreacted regions with DI water. The exposure energy and exposure time should be optimized to make sure that no PEG remained inside the microholes. The cross linking of PEG layer on alumina surface was achieved by the covalent coupling method [21-23]. The surface tethered methacrylate groups created by silane modification were capable of covalent bonding with PEG-DA during the free radical induced photoreaction (Fig. 2). Immersing hydroxylated alumina surfaces into TPM silane solution formed a dense network of Al-O-Si bonds on the substrates. This silanization process generated the methacrylate reactive groups on the substrate for further graft polymerization. When PEG-DA was exposed to UV light in presence of photoinitiator, acrylate groups formed free radical sites which reacted with TPM silane.

2.5 Surface characterization

The formation of TPM layer on nanoporous alumina surface was characterized by water contact angle measurement. The static contact angles of water droplets were measured by the sessile drop method using a contact angle goniometer (Rame-hart

model 250-F1 standard goniometer, rame-hart instrument co., USA) [24-25]. The samples were placed in a vacuum oven overnight to thoroughly remove water content of alumina before measurement. A water droplet was placed in the center of the membrane surfaces during the measurement. Contact angles on both sides of the water droplet were measured and averaged. The values reported are averages of ten measurements made on different areas of each specimen at room temperature.

Protein adsorption experiments were explored to future analyze the surface modification effects. Rhodamine-labelled fibronectin or bovine serum albumin (BSA) was dissolved in phosphate-buffered saline (PBS) (Sigma) at 50μg/ml. The substrates were washed by PBS and then immersed in the rhodamine-labelled fibronectin or BSA solution for 2 h at room temperature. After being washed three times with PBS buffer and rinsed with DI water, the samples were observed with a fluorescence microscope (Nikon 80i fluorescence microscope, Nikon, Japan).

The pore structures of nanoporous alumina samples were observed by scanning electron microscopy (SEM). The alumina samples were sputtered with a 10 nm gold layer. Then, the samples were imaged in the SEM at a voltage of 20 kV with various magnifications (JEOL, JSM-63335F, Japan).

2.6 Cisplatin release measurement

The diffusion studies for the anti-cancer drug molecule of cisplatin (300.1 Da) were carried out using a mini-diffusion chamber. A mini-diffusion chamber was

designed and fabricated using Teflon. The chamber consists of A and B compartments with fixed volume of 10 ml. The microfabricated membrane array was placed between the two compartments and screwed together (Fig. 3). Compartment A was filled with 50 μM cisplatin dissolved in PBS buffer and compartment B was filled with PBS buffer only. The donor compartment A is filled with solution of interest and the recipient compartment is filled with PBS buffer only. 100 μl samples were taken from the recipient chamber at the regular time intervals for absorbance measurement. After each sampling, the recipient compartment volume was restored to 10 ml by adding 100 μl PBS buffer. Cisplatin concentration was determined by means of ultraviolet spectroscopy (Hewlett Packard 8453 UV–VIS spectrophotometer). The measurements of each sample were repeated 5 times. Intensities of the maximum absorbance of cisplatin (λ = 301 nm) were converted to the corresponding concentration by calibration. The concentration in compartment A is treated as an infinite source C_∞. Release volume is expressed as C/C_∞ with the change of time for normalized membrane area.

2.7 Cancer cell culture and morphology

Human KYSE-30 esophageal squamous epithelial cancer cell line was obtained from American Type of Culture Collection (ATCC). KYSE-30 cells were maintained routinely in Dulbecco's Modified Eagle Medium (DMEM) with 4,500mg/L glucose (Invitrogen) as basic medium supplemented with 5% Fetal Bovine

Serum (FBS, Invitrogen) together with penicillin and streptomycin (Invitrogen). They were cultured on a 35mm diameter tissue culture dish (Nunc GmbH & Co. KG, Germany) in a humidified incubator at 37^{o}C with 5% CO_2/ 95% air. The culture medium was exchanged three times per week and routine subculturing of confluent cell layer was performed using standard trypsinization (0.05% (w/v)/ 1.5 mM EDTA) techniques. The cells were seeded on patterned alumina surfaces treated with fibronectin and cultured in the incubator. Phalloidin (Invitrogen) and propidium iodide (Invitrogen) were used to stain cytoskeletal stress fibers structure and nuclei of cells respectively.

KYSE-30 cancer cell morphology after adhesion was further examined using SEM. The cells were first fixed on the alumina membranes in 3% glutaraldehyde in 0.1M phosphate buffer for 2 h and dehydrated in a graded series of ethanol (35%, 50%, 70%, 95% and 100%) for 10 min each and then air dried for 24h. Then, the samples were sputtered with a gold layer of 10 nm and observed at a voltage of 20V using a JEOL, JSM-63335Fc SEM.

3 Results and Discussion

3.1 Fabricated chip with nanoporous alumina membrane

The microchip with nanoporous alumina membrane was successfully fabricated following the steps described in Methods. The average nanopore size diameter is around 25 nm and 55 nm. In the study, 3-(Trimethoxysilyl)propyl methacrylate (TPM)

was used to modify nanoporous alumina membrane to form a hydrophobic monolayer on the surface as described with details in Methods. The TPM monolayer could help PEG hydrogel attach to the alumina surface through the reaction of acrylate groups. The fabricated PEG microstructures were firmly anchored to the alumina surface by TPM monolayers. The reaction process is shown in Fig.2.

3.2 Fabrication of PEG hydrogel microstructures on nanoporous alumina membrane

A photomask of a 10x10 array with a diameter of 500 μm was used to fabricate the PEG hydrogel negative patterns by UV initiated polymerization. Hydrogel microstructures were successfully fabricated on the TPM self-assembled nanoporous alumina membrane (Fig. 4a). Each microwell was surrounded by PEG hydrogel and the height of microwell was approximately 15 μm which was controlled by the pre-fabricated SU-8 chamber (Fig. 4b). The unreacted PEG macromer was washed away by DI water and the clear spatial distribution of hydrophilic PEG and hydrophobic nanoporous alumina membrane was created. The PEG microstructures were anchored by TPM monolayer on the alumina membrane which was more stable than the physical adsorption method. The image of fluorescence-labeled BSA adsorption circle pattern was also shown in Fig. 4c which was achieved by the different protein adsorption capabilities between PEG and silane modified nanoporous alumina membrane. For the drug release purpose, the nanopores of the membrane should be open, and thus clogging of the pores by PEG during the fabrication was

explored. Based on the SEM images after the silane modification and PEG photopolymerization (Fig. 4d), the "open" pores were exposed to outside and the fabrication process didn't change the nanopore structure of the membrane. Clear 3-D hydrogel microwells with non-clogged pores on the bottom nanoporous alumina membranes were observed.

3.3 Protein adsorption analysis and water contact angle measurement

Surface modification was essential for the fabrication of hydrogel microwells with good adhesion on nanoporous alumina surface. To visualize the spatial surface modification effects, the water contact angle measurements and the interaction of modified membranes with fluorescence-labeled fibronectin were explored respectively.

The surface modification of nanoporous alumina membranes is characterized by water contact angle measurement. The water contact angels of unmodified nanoporous alumina membrane, PEG hydrogel, and silane modified nanoporous alumina membrane are measured. In Fig. 5, the unmodified nanoporous alumina membrane is hydrophilic with the water contact angle close to zero. The water contact angle of PEG surface is around 22^{o}. The silane-modified nanoporous alumina surface has the largest angle which is more than 130°. For protein adsorption experiment, the fluorescence-labeled fibronectin adsorption on silane modified nanoporous alumina surface is set as 100%. Unmodified nanoporous alumina surface and PEG

surface have much lower fibronectin adsorption compared with silane modified nanoporous alumina surface, which are around 18% and 28%, respectively (Fig. 5).

The big difference in fibronectin adsorption is observed between PEG and TPM silane modified nanoporous alumina surfaces. So if Extracellular Matrix (ECM) protein such as fibronectin is deposited on the microfabricated PEG-nanoporous membrane array, the difference in ECM protein adsorption between the PEG hydrogel surface and the silane modified alumina surface inside the microwell can result in cell attachment. Cells will mostly adhere on the surface inside the microwell which is discussed in next section.

3.4 Cell patterning

The PEG hydrogel micropatterns on the silane modified nanoporous alumina membrane caused hydrophobic or hydrophilic patches on the chip, which would attract or repel cells. The substrates with patterned PEG microwells were first treated with fibronectin and then incubated with KYSE-30 cancer cells. After one day incubation with cells, the alumina membrane was removed from cell culture media and then briefly washed with PBS buffer. Finally, the cells were stained and observed using a fluorescence microscopy. Fig. 6a and 6b show the fluorescent images before and after cancer cells seeding and incubation after 1 day. The difference of cell adhesion between PEG hydrogel and TPM modified nanoporous alumina surface

enabled the spatial control of cells patterning. Fig. 6c shows the SEM image of adherent KYSE-30 cancer cell on the nanoporous alumina surface.

3.5 Cisplatin diffusion

The diffusion studies for the anti-cancer drug molecule of cisplatin were carried out for the microfabricated membrane array using a mini-diffusion chamber. Compared with 25 nm and 55 nm nanopore, cisplatin is a small molecule with the molecular diameter under 1 nm. The Fick's diffusion behavior should be observed for cisplatin diffusion, i.e., the geometry of the nanopore size does not constrain the diffusion of the molecules. The process of one species across a membrane in the diffusion chamber with two compartments A and B could be described by the Fick's first law of diffusion:

$$J = D_{eff} A_{eff} \frac{C_A - C_B}{L} \qquad (1)$$

Where, J is the molar flux, D_{eff} is the effective diffusion coefficient, A_{eff} is the cross section pore area, L is the membrane thickness, and C is the concentration in the compartments .

In this experiment, there is no big difference for the diffusion coefficient of cisplatin D_{eff} for the two kinds of nanoporous membranes since the relatively large pore will not limit the diffusion of small cisplatin molecules. However, in the fabrication process of this paper, the pore cross section area A_{eff} is proportional to

the square of the pore size d^2, thus A_{eff} increases with the square of the pore size d^2. If the other conditions are the same, the diffusion rate of the cisplatin for the nanoporous membrane of 55nm is much larger than that of nanoporous membrane with the size of 25 nm. Fig. 7 shows the cisplatin diffusion curve through nanoporous alumina membrane with pore size 25 nm and 55 nm. At the initial stage of diffusion, the release volume increases linearly with time, where the slope of the curve is the diffusion rate *J*. The diffusion rates for both 25 nm and 55nm don't change much due to the stable concentration difference according to the Fick's diffusion model in Eq. 1. The slope of 55 nm is 4 to 5 times of that of 25 nm. Then, with the lapse of diffusion time, it is observed that the slope of curve (i.e. the diffusion rate) for 55 nm become smaller after 40 minutes and the slope for 25 nm almost keeps unchanged for the whole release curve (Fig. 7). It can be explained that the concentration difference (C_A-C_B) for larger pore size of 55 nm decreases faster than that of 25 nm. The experiment results in Fig. 7 agree quite well with the diffusion model based on Fick's first law. Generally, larger pore size of 55nm has faster drug release curve of cisplatin. Using larger pore size of 55 nm, complete release of small molecules of cisplatin could be achieved within a few hours.

3.6 Cell based microarray for anti-cancer drug effects study

In this experiment, the well established anti-cancer drug of cisplatin was used to explore the effects on KYSE-30 cancer cells using the microfabricated membrane

array with the pore size of 55 nm. The cells were first seeded on the patterned alumina surface treated with fibronectin and cultured in the incubator for 3 days. Then, soft washing was followed by PBS solution. The diffusion chamber was established as described in Section 3.5 using the microfabricated membrane array with adherent cancer cells. Then, the cisplatin drug was added to the chamber without cells at a concentration of 50 μM. Due to the concentration difference between the two compartments, the drug molecules were diffused through the nanopores and interacted with the adherent cancer cells on the nanoporous membrane. The cancer cells were exposed to the cisplatin diffused through the nanoporous membrane from 15 minutes to 7 hours and then cultivated in fresh medium without drug in incubator for 12 hours. At the end of each incubation experiment, the cells were stained and counted under a fluorescence microscope.

With respect to cisplatin release through the nanoporous membrane, the drug was extracted from the medium of the cell exposure chamber at different time and quantified by an UV–VIS spectrophotometer. The controlled drug released profile was achieved and the drug concentration reached a plateau within 7 hours (Fig. 8). Compared with the cisplatin diffusion curve without cells shown in Fig. 7, the drug release rate was apparently lower in the first two hours due to the partial covering of the nanopores by the adherent cells. We also explored the cytotoxic effect of cisplatin on the KYSE-30 cancer cells with 12h culture in normal medium after the cells were exposed to cisplatin released through the nanopores at different time points. A clear anti-proliferation effect was observed in Fig. 8, where the adherent cancer cell number

per microwell decreased with the drug release time due to increased cisplatin concentration.

The cellular morphology changes during the cisplatin diffusion were studied by fluorescence microscopy. Cellular morphology is one of the most important parameters in anti-cancer drug chemotherapeutics. The cytoskeleton consists of a complex network of filamentous proteins which are involved in regulation of cell morphology and adhesion. Most anti-cancer agents which target cytoskeleton such as cisplatin, modulate the cell morphology by interacting with the microfilaments [26]. Cisplatin inhibits cancer cell-substrate adhesion and also induces cell morphological changes such as cell rounding [27-30]. Fig. 9a shows the fluorescence image of stained KYSE-30 cancer cells immobilized on the PEG-alumina based micro-array chip. It could be observed that the cell spreading was confined within the microwells. The fluorescence image stained for nuclei was also shown in Fig. 9b where the cell number within each microwell could be counted. Fig. 9c shows the enlarged fluorescence image stained for stress fibers of cytoskeleton structure. In the absence of cisplatin, the cells anchored well to the surface and showed good cell spreading with prominent stress fibers within each microwell. Cell detachment and morphology after cisplatin treatment could also be examined by the fluorescence microscopy. Fig. 9d and 9e shows the microwell array with KYSE-30 cancer cells at 7 h exposure to cisplatin diffused through nanoporous membrane (C_{∞}=50μM). A marked cell detachment was observed after cisplatin exposure. The detached cells left the growth surface due to the loss of cell-substrate contacts. A series of characteristics

including loss of cell volume, reconstructing of actin fibers, shrinkage of cell spreading area and even round-up of cells were observed in the enlarged fluorescence image (Fig. 9f).

4. Conclusion

The present paper outlines a microfludic system with PEG hydrogel micro-arrays on nanoporous alumina membrane on a silicon chip for cell drug interaction analysis. The PEG hydrogel microwells were fabricated on the silane modified nanoporous alumina surface with controlled spatial distribution of hydrophobic and hydrophilic regions. ECM proteins were selectively deposited on the nanoporous membrane within PEG microwells. KYSE-30 cancer cells were then successfully patterned within the microwells to form cell microarrays. For demonstration, anti-cancer drug cisplatin was used as a model drug for diffusion experiments to explore the effect on cancer cell adhesion and morphology. The nanoporous membranes acted as a cell interface for culturing and modulated the cell environment by well controlled drug delivery. The integration of nanoporous alumina membranes on a microfabricated silicon chip avoided the brittleness of pure alumina membrane and allowed integration other functions for further development.

Acknowledgement

This work was supported by the Hong Kong Research Council General Research Grant (B-Q07N) and Internal Research Grant of the Hong Kong Polytechnic University (G-YG91).

References

[1] T. Satomi, Y. Nagasaki, H. Kobayashi, H. Otsuka, K. Kataoka., Density control of poly(ethylene glycol) layer to regulate cellular attachment, Langmuir, 23 (2007) 6698.

[2] N.L. Jeon, H. Baskaran, S.K.W. Dertinger, G.M. Whitesides, L.V.D. Water, M. Toner, Neutrophil chemotaxis in linear and complex gradients of interleukin-8 formed in a microfabricted device, Nature biotechnology, 20 (2002) 826.

[3] A. Revzin, R.G. Tompkins, M. Toner, Surface engineering with poly(ethylene glycol) photolithography to create high-density cell arrays on glass, Langmuir, 19 (2003) 9855.

[4] K. Itaya, S. Sugawara, K. Arai, S. Saito, Properties of porous anodic aluminum oxide films as membranes, J. Chem. Engr. Jpn. 17 (1984) 514.

[5] S. Tajima, Advances in Corrosion Science and Technology 1 (1970) 229.

[6] K. Itaya, S. Sugawara., K. Arai, S. Saito., Properties of porous anodic aluminum oxide films as membranes, J. Chem. Eng. Japan. 17 (1984) 514.

[7] Y. Xu., G.E. Thompson, G.C. Wood, Mechanism of anodic film formation on aluminium, Trans. Inst. Met. Finish. 63 (1985) 98..

[8] H. Masuda, F. Hasegawa, S. Ono, Self-ordering of cell arrangement of anodic porous alumina formed in sulfuric acid solution, J. Electrochem. Soc. 144 (1997) 127–129

[9] O. Jessensky, F. Müller and U. Gösele, Self-organized formation of hexagonal pore arrays in anodic alumina, Appl. Phys. Lett. **72** (1998) 1173.

[10] S.Y. Zhao, H. Roberge, A. Yelon, T. Veres, New application of AAO template: a mold for nanoring and nanocone arrays, J. Am. Chem. Soc. 128 (2006) 12352.

[11] W. Chen, J.H. Yuan, X.H. Xia, Characterization and manipulation of the electroosmotic flow in porous anodic alumina membranes, Anal. Chem., 77 (2005) 8102.

[12] I. Vlassiouk, A. Krasnoslobodtsev, S. Smirnov, M. Germann, 'Direct' detection and separation of DNA using nanoporous alumina filters, Langmuir, 20 (2004) 9913.

[13] I. Vlassiouk, P. Takmakov, S. Smirnov, Sensing DNA Hybridization via Ionic Conductance through a Nanoporous Electrode, Langmuir, 21 (2005) 4776.

[14] P. Takmakov, I. Vlassiouk, S. Smirnov, Hydrothermally shrunk alumina nanopores and their application to DNA sensing, Analyst, 131 (2006) 1248.

[15] L. Leoni, A. Boiarski, T.A. Desai, Characterization of nanoporous membranes for immunoisolation: Diffusion properties and tissue effects, Biomedical Microdevices 4 (2002) 131.

[16] K.C. Popat, P. Mor, C.A. Grimes, T.A. Desai, Surface modification of nanoporous alumina surfaces with poly(ethylene glycol), Langmuir 20 (2004) 8035.

[17] K.C. Popat, E.E.L. Swan, V. Mukhatyar, K.I. Chatvanichkul, G.K. Mor, C.A. Grimes, T.A. Desai, Peptide-immobilized nanoporous alumina membranes for enhanced osteoblast adhesion, Biomaterials, 26 (2005) 4516.

[18] V. Szczepanskia, I. Vlassiouka, S. Smirnov, Stability of silane modifiers on alumina nanoporous membranes, Journal of Membrane Science, 281 (2006) 587.

[19] D.J. Odom, L.A. Baker, C.R., J. Martin, Solvent-extraction and langmuir-adsorption-based transport in chemically functionalized nanopore, J. Phys. Chem. B, 109 (2005) 20887.

[20] E.D. Steinle, D.T. Mitchell, M. Wirtz, S.B. Lee, V.Y. Young, C.R. Martin, Ion channel mimetic micropore and nanotube membrane sensors, Anal. Chem. 74 (2002) 2416.

[21] S. Park, Y.S. Chi, I.S. Choi, J. Seong, S. Jon, A facile method for construction of antifouling surfaces by self-assembled polymeric monolayers of PEG-silane copolymers formed in aqueous medium, J. Nanosci. Nanotechnol. 6 (2006) 3507.

[22] W. Zhan, G. H. Seong, R.M. Crooks, Hydrogel-based microreactors as a functional component of microfluidic systems, Anal. Chem. 74 (2002) 4647.

[23] W.G. Koh, A. Revzin, A. Simonian, T. Reeves, M. Pishko, Control of mammalian cell and bacteria adhesion on substrates micropatterned with poly(ethylene glycol) hydrogels, Biomedical Microdevices, 5 (2003) 11.

[24] P.S. Cheow, L.Y Liu, C.S. Toh, Grafting of nanoporous alumina membranes and films with organic acids, Surf. Interface Anal. 39 (2007) 601.

[25] C.B. Ran, G.Q. Ding, W.C. Liu, Y. Deng, W.T. Hou, Wetting on nanoporous alumina surface: transition between wenzel and cassie states controlled by surface structure, Langmuir, 24 (2008) 9952.

[26] P. Köpf-Maier, S.K. Mühlhausen, Changes in the cytoskeleton pattern of tumor cells by cisplatin in vitro, Chem Biol Interact. 82 (1992) 295.

[27] H. Sasaki, F. Kotsuji, B.K, Tsang. Caspase 3-mediated focal adhesion kinase processing in human ovarian cancer cells: possible regulation by X-linked

inhibitor of apoptosis protein, Gynecologic Oncology, 85 (2002) 339.

[28] RG. Deschesnes, A. Patenaude, JLC. Rousseau, JS. Fortin, C. Ricard, M.F. Cote MF, J. Huot, R.C. Gaudreault, E. Petitclerc, Microtubule-destabilizing agents induce focal adhesion structure disorganization and anoikis in cancer cells, The Journal of Pharmacology and Experimental Therapeutics, 320 (2007) 853.

[29] SA. Park, HJ. Park, BI. Lee, YH. Ahn, SU. Kim, KS. Choi, Bcl-2 blocks cisplatin-induced apoptosis by suppression of ERK-mediated p53 accumulation in B104 cells, Molecular Brian Research, 93 (2001) 18.

[30] YH. Zeidan, RW. Jenkins, YA. Hannun, Remodeling of cellular cytoskeleton by the acid sphingomyelinase/ceramide pathway, the Journal of Cell Biology, 181 (2008) 335.

Fig. 1 Process flow for the fabrication of PEG hydrogel microarrays on nanoporous alumina membrane based on a silicon substrate.

Fig. 2 Schematic view of the silanization and PEG grafting process on nanoporous alumina surface.

Fig. 3 Mini-diffusion chamber setup used to test the microfabricated membrane array.

Fig. 4 (a) The 10x10 microwells array on the modified nanoporous membrane; (b) Scanning electron microscopy image of 3-D hydrogel microwells with nanoporous membrane in the bottom; (c) Fluorescent BSA adsorption micro-patterns; (d) "Open" nanopores were observed in the microwells.

Fig. 5 Water contact angle and fluorescence labeled fibronectin adsorption measurements on three kinds of substrates: unmodified nanoporous alumina surface (contact angle: 6±0.4^{o}, protein adsorption: 18%), PEG hydrogel surface (contact angle: 22±1.6^{o}, protein adsorption: 28%) and TPM silane modified nanoporous alumina surface (contact angle: 132±7.2^{o}, protein adsorption: 28%). For fibronectin adsorption measurement, the intensities were normalized using that of the silane modified nanoporous alumina surface (100%).

Fig. 6 (a) Fluorescence image of cancer cell patterning before and (b) after cancer cells seeding for one day, (c) SEM image of adherent KYSE-30 cancer cell on the nanoporous alumina surface.

Fig. 7 Normalized release curve of cisplatin diffused through the microfabricated membrane array with the pore size of 25 nm and 55 nm.

Fig. 8 Controlled release curve of cisplatin through the microfabricated membrane array with cultured KYSE-30 cancer cells and cytotoxicity of cisplatin referred to the adherent cell number change within microwells (n=5). The nanopore size of the tested membrane array is 55 nm.

Fig. 9 Fluorescence images for cell based microarray before and after addition of cisplatin. (a) Cellular microarray with phalloidin staining for microfilament, (b) cellular microarray with propidium iodide staining for nuclei, and (c) enlarged fluorescence image stained for stress fibers of cytoskeleton structure after KYES30 cancer cells cultured on the microfabricated membrane array after 3 days incubation; (d) Cellular microarray with phalloidin staining for microfilament, (e) propidium iodide staining for nuclei, and (f) enlarged fluorescence image stained for stress fibers of cytoskeleton structure after KYSE-30 cancer cells at 7h exposure to cisplatin diffused through nanoporous alumina membrane (C_{∞}=50μM).

Figure 1

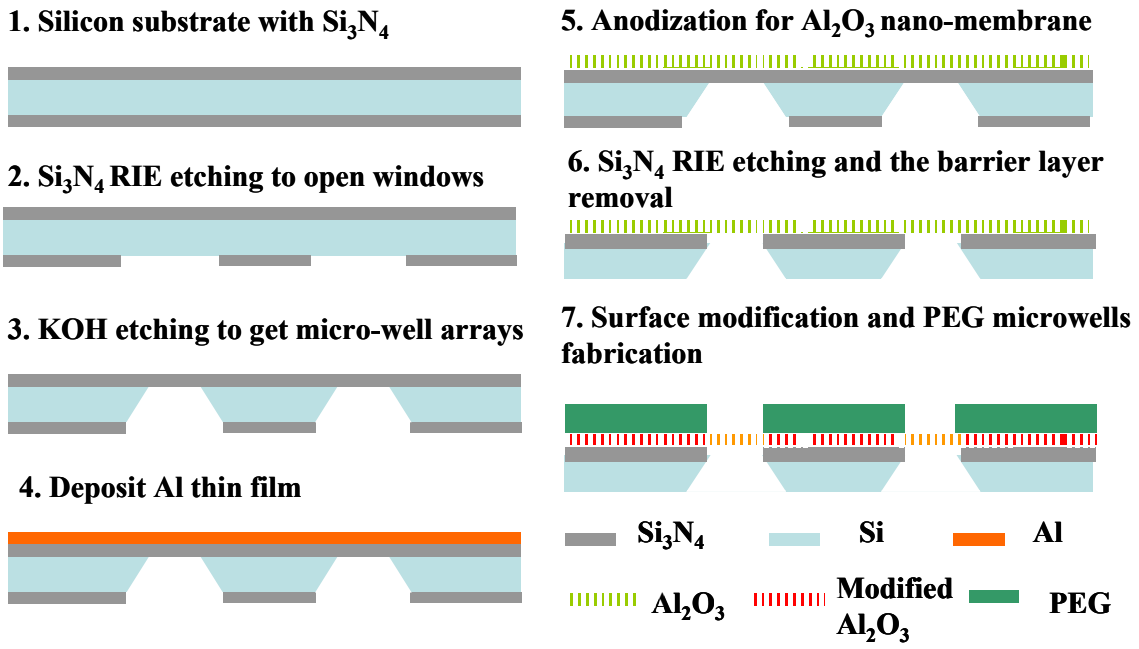
1. Silicon substrate with Si_3N_4
2. Si_3N_4 RIE etching to open windows
3. KOH etching to get micro-well arrays
4. Deposit Al thin film
5. Anodization for Al_2O_3 nano-membrane
6. Si_3N_4 RIE etching and the barrier layer removal
7. Surface modification and PEG microwells fabrication
Si_3N_4
Si
Al
Al_2O_3
Modified Al_2O_3
PEG

Figure 2

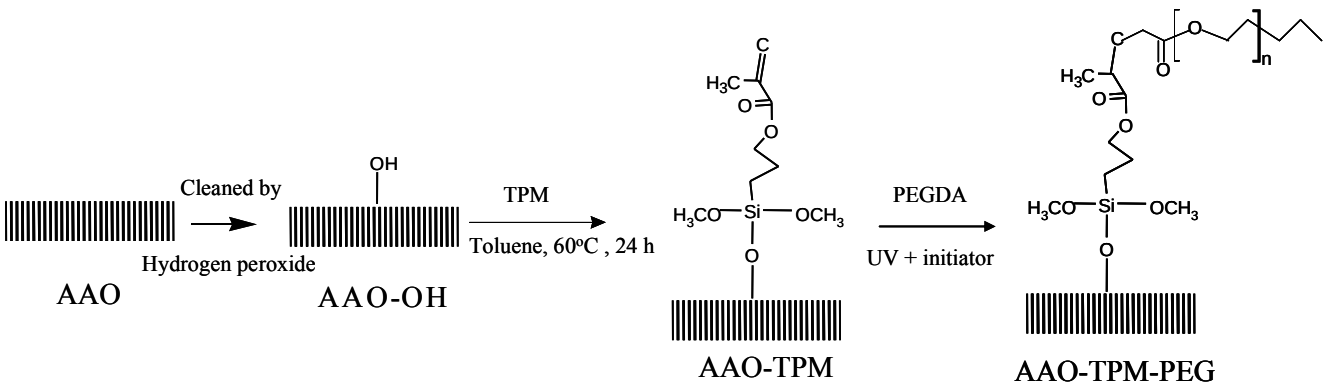
Cleaned by
Hydrogen peroxide
OH
AAO
AAO-OH
TPM
Toluene, 60°C , 24 h
AAO-TPM
PEGDA
UV + initiator
AAO-TPM-PEG

Figure 3

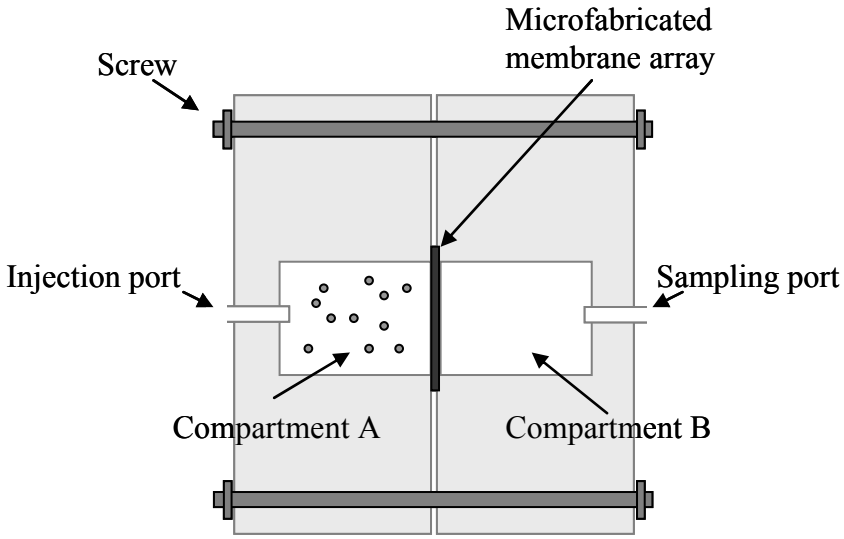
Microfabricated
membrane array
Screw
Injection port
Sampling port
Compartment A
Compartment B

Figure 4

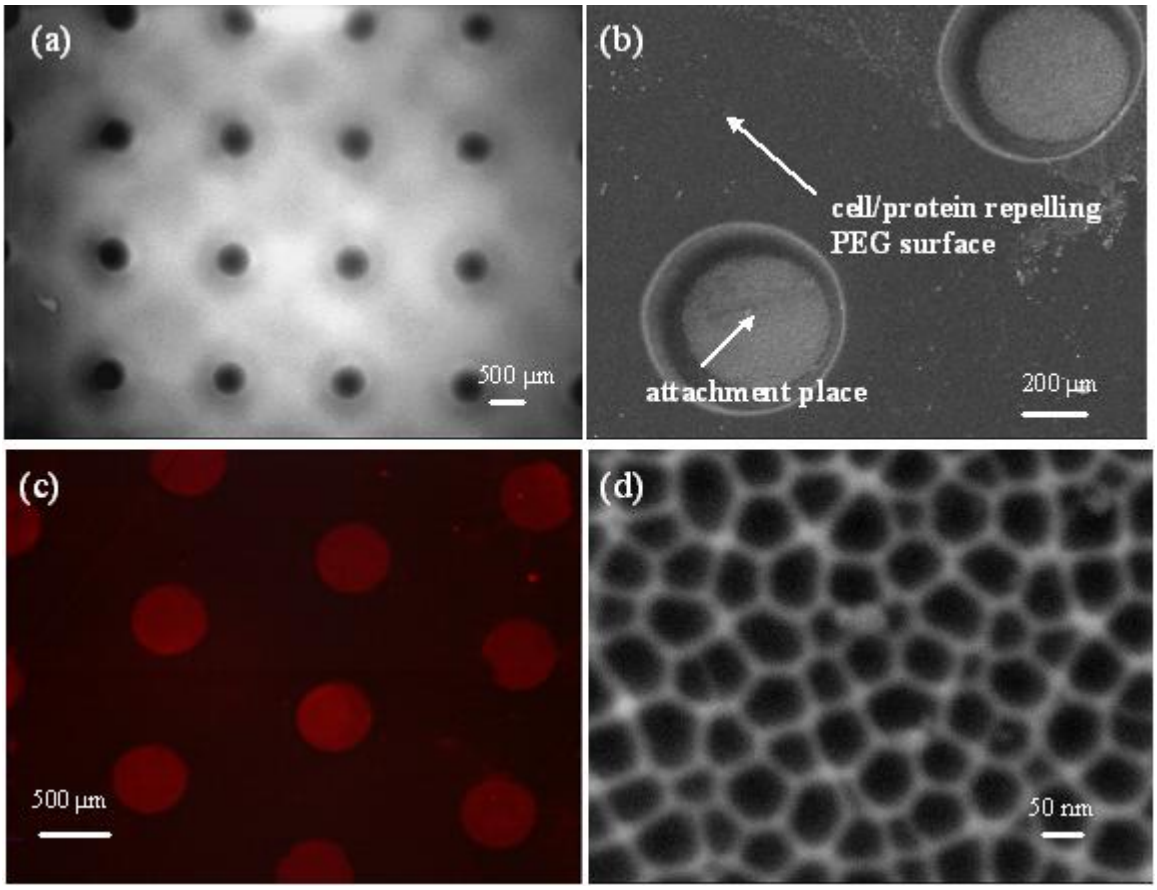
(a)
500 µm
(b)
cell/protein repelling
PEG surface
attachment place
200 µm
(c)
500 µm
(d)
50 nm

Figure 5

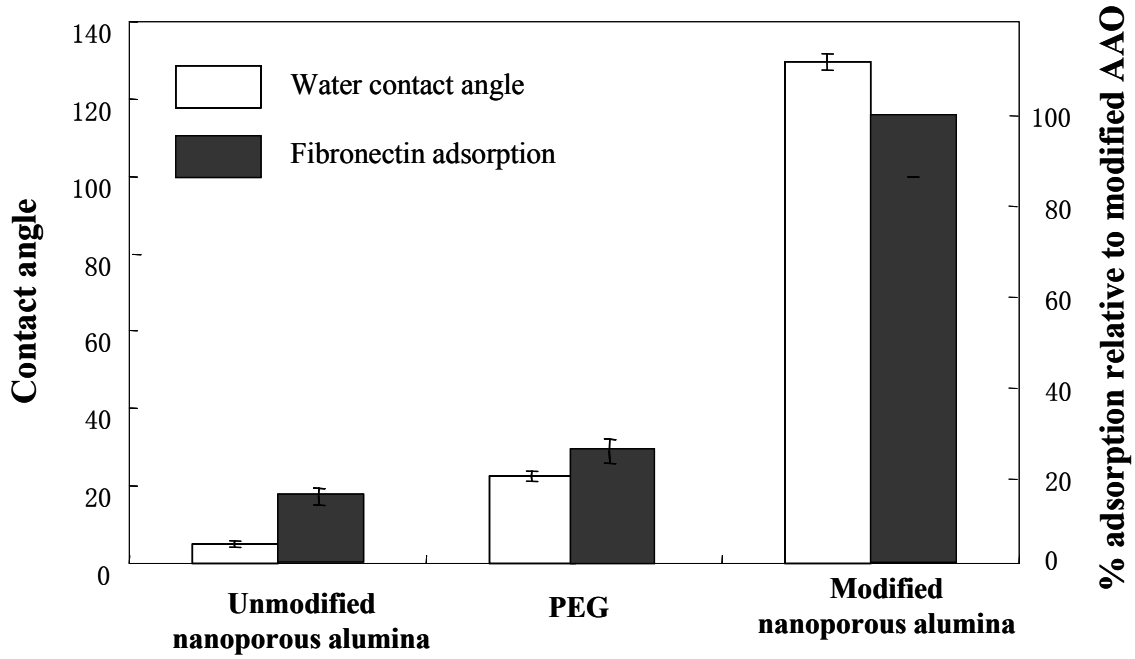
Water contact angle
Fibronectin adsorption
Contact angle
% adsorption relative to modified AAO
140
120
100
80
60
40
20
0
100
80
60
40
20
0
Unmodified nanoporous alumina
PEG
Modified nanoporous alumina

Figure 6

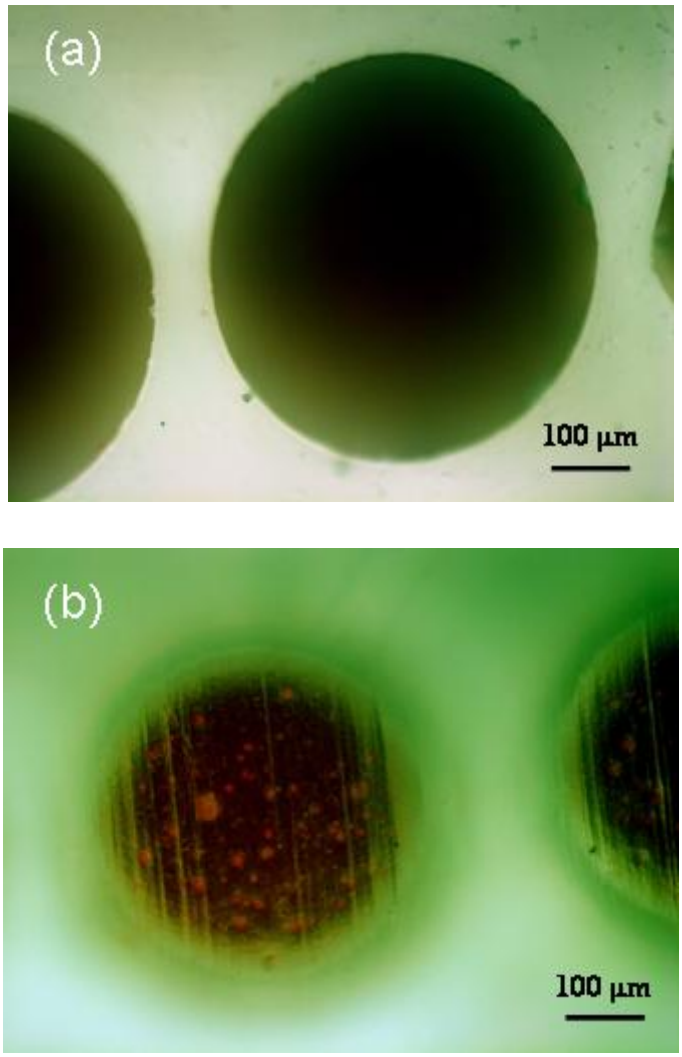
(a)
100 µm
(b)
100 µm
(c)
2 µm
MAG = 20.00 K X
EHT = 20.00 kV
2µm
Detector = SE1
Date :21 May 2007

Figure 7

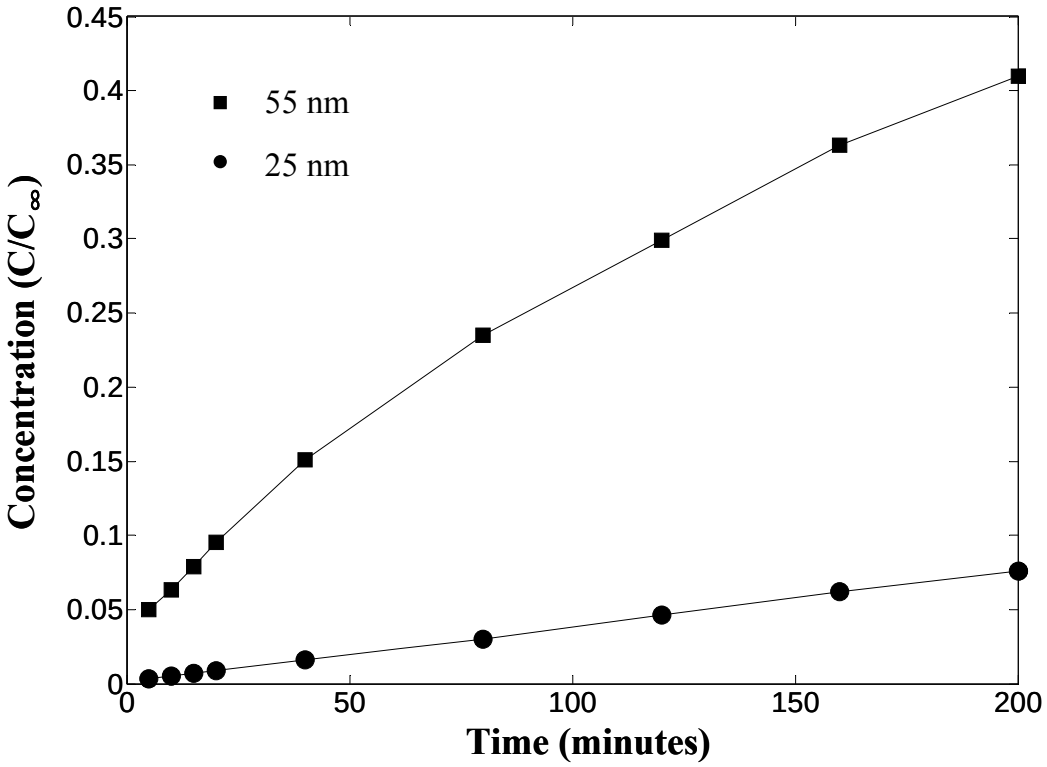
0.45
0.4
0.35
0.3
0.25
0.2
0.15
0.1
0.05
0
0
50
100
150
200
55 nm
25 nm
Concentration (C/C∞)
Time (minutes)

Figure 8

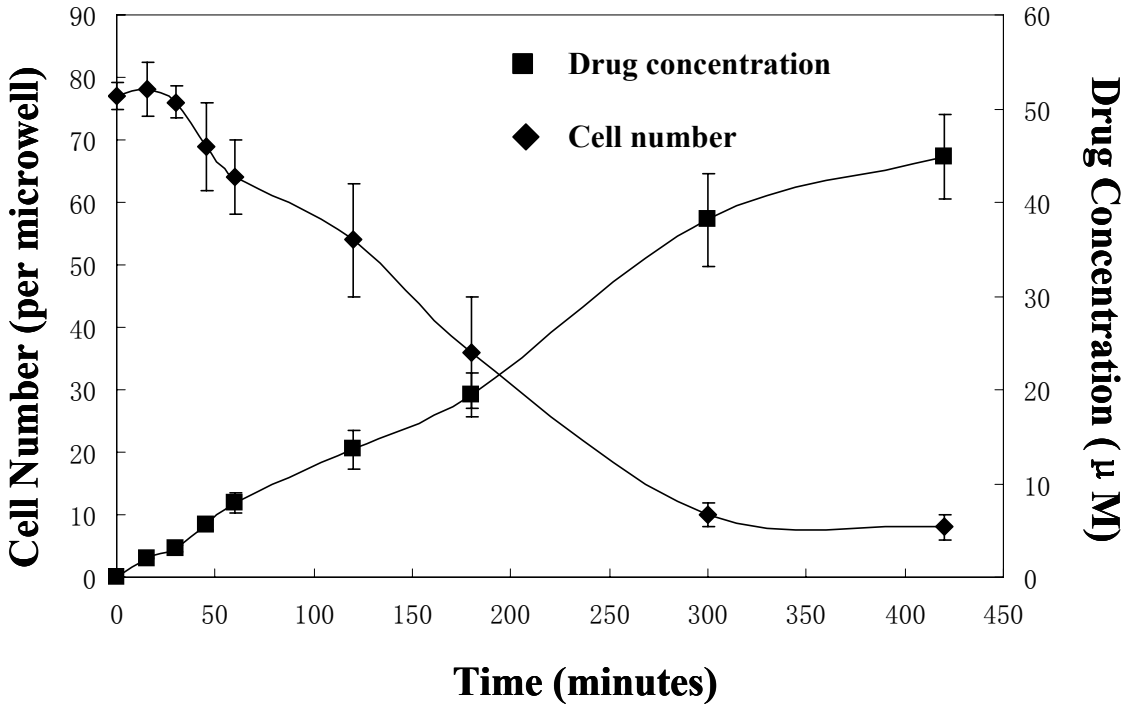
Drug concentration
Cell number
Cell Number (per microwell)
Drug Concentration (μ M)
Time (minutes)
0
10
20
30
40
50
60
70
80
90
0
50
100
150
200
250
300
350
400
450

Figure 9